

Diode-pumped composite $\text{YVO}_4/\text{Nd:YVO}_4/\text{YVO}_4$ self-Raman second-Stokes laser at 1764 nm

Xiaohua Xie (谢晓华)^{1,2,3}, Yongqin Yu (于永芹)^{2,3,4}, Yufeng Zhang (张玉凤)^{1,2,3},
Dong Wang (王冬冬)^{1,2,3}, and Chenlin Du (杜晨林)^{1,2,3*}

¹College of Electronic Science and Technology, Shenzhen University, Shenzhen 518060, China

²Shenzhen Key Laboratory of Laser Engineering, Shenzhen University, Shenzhen 518060, China

³Key Laboratory of Advanced Optical Precision Manufacturing Technology of Guangdong Higher Education Institutes, Shenzhen University, Shenzhen 518060, China

⁴College of Physics Science and Technology, Shenzhen University, Shenzhen 518060, China

*Corresponding author: cldu@szu.edu.cn

Received January 15, 2014; accepted March 15, 2014; posted online October 14, 2014

We report a diode-end-pumped Q-switched $\text{YVO}_4/\text{Nd:YVO}_4/\text{YVO}_4$ self-Raman second-Stokes laser at the wavelength of 1764 nm. With the incident pump power of 32 W and the pulse repetition frequency of 20 kHz, the maximal average output power at 1764 nm is up to 1.18 W, with the corresponding optical conversion efficiency of 3.69%. The highest pulse energy and peak power are 59 μJ and 31.7 kW, respectively.

OCIS codes: 140.3550, 140.3540, 140.3480, 140.3580, 140.3530.

doi: 10.3788/COL201412.S21405.

Neodymium-doped yttrium vanadate crystal, such as Nd:YVO_4 and Nd:GdVO_4 crystal, has been considered as a wonderful Raman medium in diode-pumped solid-state lasers. To date, Nd:YVO_4 crystal has been widely employed in actively Q-switched Raman lasers^[1-4]. In these studies, major attention was focused on the first-Stokes Raman laser operating at the wavelengths of $\lambda_{\text{St1}} = 1176$ and 1525 nm. In recent years, Chen *et al.*^[5,6] successively reported the second-Stokes self-Raman laser operating at the wavelength of $\lambda_{\text{St2}} = 1313$ nm. However, the second-Stokes self-Raman laser at $\lambda_{\text{St2}} = 1764$ nm has been rarely reported.

As we all know, the laser sources operating at the eye-safe region of the spectrum (1.4–1.8 μm) are of great interest for various potential applications such as laser ranging, remote sensing, and active imaging. The methods of generating 1.7 μm laser include optical parametric oscillator (OPO)^[7,8], Er^{3+} -doped crystal solid-state laser^[9], and stimulated Raman scattering (SRS). Among these methods, the self-Raman lasers with the advantages of compact structure and high efficiency have attracted more and more attention. The disadvantage of OPO is either the complex experimental setup or the necessary special crystal temperature control. Compared with 1.7 μm non-Raman lasers, the Raman lasers have a number of unique characteristics including Raman beam cleanup and pulse-shortening^[10-12].

Here a diode-end-pumped actively Q-switched second-Stokes $\text{YVO}_4/\text{Nd:YVO}_4/\text{YVO}_4$ self-Raman laser at 1764 nm was demonstrated. The maximum output power at 1764 nm was up to 1.18 W at the pump power of 32 W and the pulse repetition frequency (PRF) of 20 kHz, with the corresponding optical conversion efficiency of 3.69%. The highest pulse energy and peak power were 59 μJ and 31.7 kW, respectively. In our work, a double-end

diffusion-bonded composite Nd:YVO_4 crystal was employed which not only mitigated the thermal effects but also increased the Raman interaction length for the SRS frequency conversion.

The experimental setup of the double-end diffusion-bonded Nd:YVO_4 self-Raman second-Stokes laser at 1764 nm is shown in Fig. 1. The pump source was a high-power fiber-coupled diode laser array at 808 nm. The core diameter and numerical aperture of the fiber were 0.4 mm and 0.22, respectively. The fiber output was focused into the laser crystal, and the spot size was 0.4 mm in diameter. The front flat mirror M1 was high transmittance (HT) coated at 808 nm and high reflection (HR) coated at 1342, 1525, and 1764 nm. A 250 mm radius-of-curvature concave mirror was employed to act as the output coupler, M2, which was HR coated at 1342 and 1525 nm and HT coated at 1764 nm. The resonator cavity length from M1 to M2 was 103 mm. The composite Nd:YVO_4 crystal was a 10-mm-long 0.3-at.% Nd^{3+} doped a-cut Nd:YVO_4 crystal bounded with a 2-mm-long pure YVO_4 at the pumped end and an 18-mm-long pure YVO_4

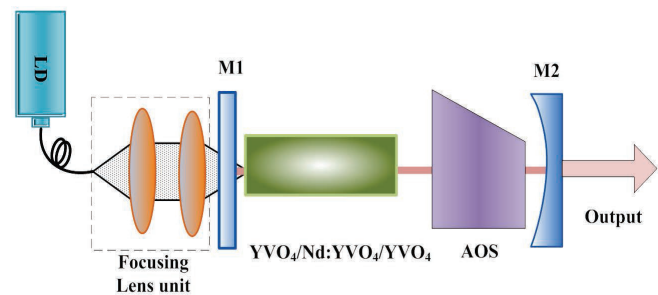


Fig. 1. Schematic diagram of the composite Nd:YVO_4 crystal second-Stokes self-Raman laser.

at another end. It was anti-reflection (AR) coated at 808, 1064, and 1342 nm on both of its faces. And the transmittances of the laser crystal at 1525 and 1764 nm were measured to be 91% and 70%, respectively. The absorption efficiency of the incident pump power was measured to be about 95%. The laser crystal was wrapped with indium foil and mounted on a water-cooled copper block heat sink. And the water temperature was kept around 20 °C. A 46-mm-long acousto-optic (AO) Q-switch (AOS, Gooch & Housego Co.) was AR coated at 1342 and 1525 nm. Its transmittance at 1764 nm was measured to be 90%. All the elements in the cavity were HT coated at 1064 nm in order to suppress parasitic oscillations at the 1.06 μm region.

SRS is a cascading nonlinear frequency conversion process. Due to the high SRS threshold, the performance of the Raman lasers depends on the intensity of the fundamental laser beam. Thus, an AO Q-switch with suitable duty cycle is essential for the operation of the Raman lasers. Hence the duty cycle of the Q-switch was optimized firstly. The output powers of second-Stokes Raman lasers at 1764 nm versus the incident pump power were measured with different PRFs of 20, 25, and 30 kHz, as shown in Fig. 2. The threshold of the second-Stokes emission for the PRFs of 20, 25, and 30 kHz were measured to be 7, 8, and 8 W, respectively. It can be seen that the second-Stokes output powers tend to saturate at the maximum level. It was due to the resonator instability caused by the strong thermal lens effect resulting from the SRS process^[13]. At the incident pump power of 32 W and the PRF of 20 kHz, the maximum average output power was up to 1.18 W, with the corresponding optical conversion efficiency of 3.69%. The highest single pulse energy and peak power were 59 μJ and 31.7 kW, respectively. At the other PRFs of 25 and 30 kHz, the maximum output powers were measured to be 1.11 and 1.04 W, with the corresponding optical conversion efficiency of 3.70% and 3.71%, respectively. There were several reasons for the low optical conversion efficiency. Firstly, the stimulated emission cross section of the Nd:YVO₄ crystal at 1342 nm was smaller than that at 1064 nm. Secondly, the laser

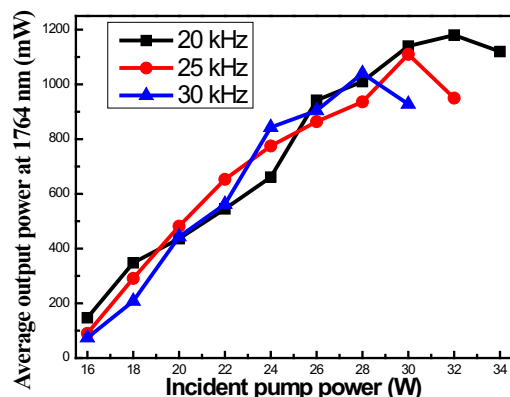


Fig. 2. Average output power at 1764 nm versus the incident pump power for different PRFs of 20 kHz, 25 kHz, and 30 kHz.

crystal and the Q-switch, which were not AR coated at 1764 nm, could lead to more loss in the cavity. Finally, higher conversion efficiency could be expected with the optimization of the output coupling. In the experiments, the fundamental, first-, and second-Stokes radiations were measured to be linearly polarized along the π -direction (electric field // c). The π -polarized radiation was beneficial for avoiding undesirable thermally induced birefringence^[14] and improving the Raman conversion efficiency^[15,16].

The spectrum information was monitored by an optical spectrum analyzer (Yokogawa AQ6375) with the resolution of 0.05 nm. The typical optical spectrum of output radiation was obtained at the incident pump power of 32 W and the PRF of 20 kHz. As shown in Fig. 3, the central wavelengths of the fundamental, first-, and second-Stokes radiations were determined to be 1342.51, 1524.74, and 1764.29 nm. The frequency shift of each adjacent wavelengths interval was in good agreement with the optical vibration mode of the tetrahedral VO₄³⁻ ionic groups (890 cm^{-1}).

In order to investigate the phenomenon of pulse-shortening in the SRS conversion process, a grating monochromator was employed to separate the fundamental, first-, and second-Stokes radiations. The temporal pulse behaviors were recorded by a mixed signal oscilloscope (Tektronix MSO 4032) connected to a fast photodiode detector (EOT ET-3500). The pulse widths versus the incident pump power at the PRF of 20 kHz are shown in Fig. 4. It can be seen that the pulse widths decrease with the increasing pump power. However, the second-Stokes pulse widths were shorter than that of the first Stokes. And the first-Stokes pulse widths were shortened significantly compared with the fundamental widths. This result indicated that the cascading SRS frequency conversion process led to pulse-shortening of the Stokes radiation. It can be expected that the pulses of higher order Stokes would have much shorter duration.

The temporal profiles of the output pulses at the pump power of 32 W and the PRF of 20 kHz are shown in Fig. 5. It can be seen that the second-Stokes

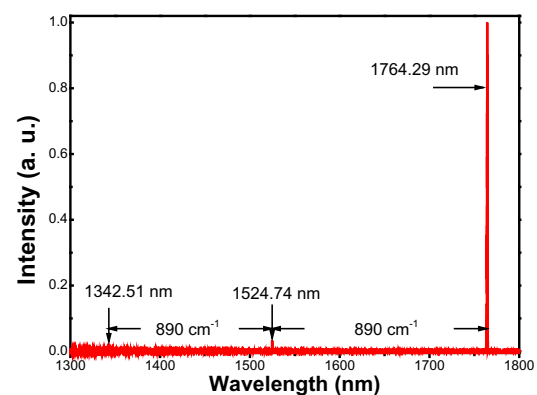


Fig. 3. The optical spectrum of the composite Nd:YVO₄ crystal second-Stokes self-Raman laser.

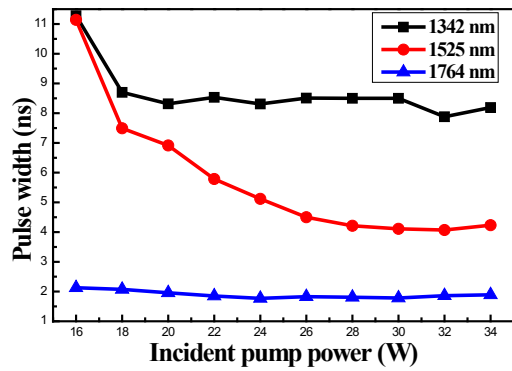


Fig. 4. Pulse widths for the output pulses versus the incident pump power at the PRF of 20 kHz.

pulse follows behind the first-Stokes pulse, which is just trailing the fundamental pulse. However, the second-Stokes pulse differs in temporal behavior from that of the fundamental and first-Stokes pulses. It is obvious that the falling edges of the fundamental and first-Stokes pulses are broadened much more. The part of the fundamental pulse that overlapped with the first-Stokes pulse was depleted by the SRS conversion, transferring power to the first-Stokes field. Then the first-Stokes field was amplified in the Raman cavity, and acted as the pump for the second-Stokes radiation. Figure 6 shows the oscilloscope traces of

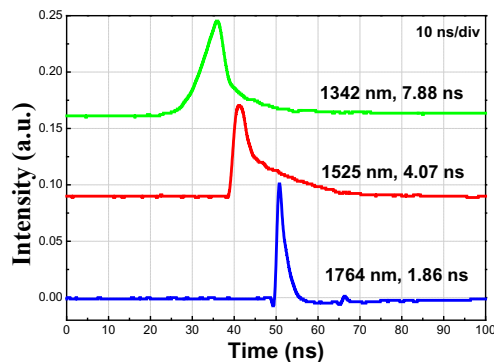


Fig. 5. Output pulses profiles at the pump power of 32 W and the PRF of 20 kHz.

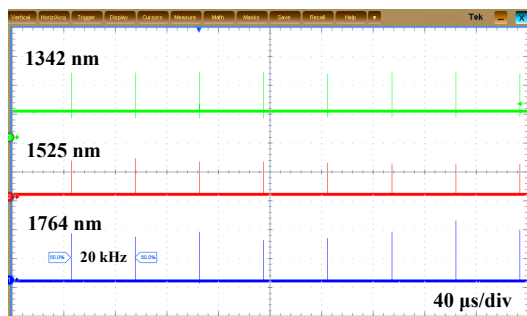


Fig. 6. Oscilloscope traces of the output pulses with the pump power of 32 W and the PRF of 20 kHz.

the output pulses for a time span of 400 μ s. It can be seen that the fundamental and the first-Stokes pulses have little fluctuation in the amplitude. However, the fluctuation of the second-Stokes pulses is more obvious than that of the first Stokes. The beam quality factor (M^2) of the second Stokes was measured to be 1.52×1.63 in the horizontal and vertical directions, respectively.

In conclusion, we demonstrate an actively Q-switched second-Stokes self-Raman laser at 1764 nm based on the composite $\text{YVO}_4/\text{Nd:YVO}_4/\text{YVO}_4$ crystal. The maximal output power at 1764 nm is up to 1.18 W with the incident pump power of 32 W and the PRF 20 kHz, with the corresponding optical conversion efficiency of 3.69%. The highest single pulse energy and peak power are 59 μ J and 31.7 kW, respectively. It is expected that a higher output power of second-Stokes radiation can be achieved with 1764 nm HT coated laser crystal and Q switch.

This work was supported by the National Natural Science Foundation of China (No. 10804074), the Science and Technology Project of Shenzhen (Nos. JCYJ20130326113421781, JCYJ20120613105141482, and JC201005280473A), and the Specialized Research Fund for the Doctoral Program of Higher Education (NO. 20124408120004).

References

1. Y. F. Chen, Opt. Lett. **29**, 2172 (2004).
2. S. H. Ding, X. Y. Zhang, Q. P. Wang, F. F. Su, P. Jia, S. T. Li, S. Z. Fan, J. Chang, S. S. Zhang, and Z. J. Liu, IEEE J. Quantum Electron. **42**, 927 (2006).
3. H. Y. Zhu, Y. M. Duan, G. Zhang, C. H. Huang, Y. Wei, H. Y. Shen, Y. Q. Zheng, L. X. Huang, and Z. Q. Chen, Opt. Express **17**, 21544 (2009).
4. C. L. Du, L. Zhang, Y. Q. Yu, S. C. Ruan, and Y. Y. Guo, Appl. Phys. B **101**, 743 (2010).
5. W. Chen, Y. Wei, C. Huang, X. Wang, H. Shen, S. Zhai, S. Xu, B. Li, Z. Chen, and G. Zhang, Opt. Lett. **37**, 1968 (2012).
6. C. L. Du, Y. Y. Guo, Y. Q. Yu, G. X. Huang, and S. C. Ruan, Laser Phys. Lett. **10**, 055802 (2013).
7. K. C. Burr, C. L. Tang, M. A. Arbore, and M. M. Fejer, Opt. Lett. **22**, 1458 (1997).
8. X. Y. Peng, L. Xu, and A. Asundi, IEEE J. Quant. Electron. **41**, 53 (2005).
9. N. Barnes, R. Allen, L. Esterowitz, E. Chicklis, M. Knights, and H. Jenssen, IEEE J. Quant. Electron. **22**, 337 (1986).
10. R. Frey, A. Demartino, and F. Pradere, Opt. Lett. **8**, 437 (1983).
11. J. R. Ackerhalt, Y. B. Band, J. S. Krasinski, and D. F. Heller, Opt. Lett. **13**, 646 (1988).
12. H. M. Pask, Prog. Quant. Electron. **27**, 3 (2003).
13. A. J. Lee, H. M. Pask, P. Dekker, and J. A. Piper, Opt. Express **16**, 21958 (2008).
14. W. Koechner, *Solid-State Laser Engineering* (Springer, 1999).
15. P. A. Fields, M. Birnbaum, and C. L. Fincher, Appl. Phys. Lett. **51**, 1885 (1987).
16. J. J. Zayhowski and C. Dill, Opt. Lett. **20**, 716 (1995).